



HAL
open science

Monitoring mechanical stimulation for optimal tendon tissue engineering: a mechanical and biological multiscale study

Alejandro Garcia Garcia, Jean-Baptiste Perot, Megane Beldjilali-Labro, Quentin Dermigny, Marie Naudot, Sophie Le Ricousse, C. Legallais, Fahmi Bedoui

► To cite this version:

Alejandro Garcia Garcia, Jean-Baptiste Perot, Megane Beldjilali-Labro, Quentin Dermigny, Marie Naudot, et al.. Monitoring mechanical stimulation for optimal tendon tissue engineering: a mechanical and biological multiscale study. *Journal of Biomedical Materials Research Part A*, 2021, 10.1002/jbm.a.37180 . hal-03029652

HAL Id: hal-03029652

<https://hal.science/hal-03029652>

Submitted on 28 Nov 2020

HAL is a multi-disciplinary open access archive for the deposit and dissemination of scientific research documents, whether they are published or not. The documents may come from teaching and research institutions in France or abroad, or from public or private research centers.

L'archive ouverte pluridisciplinaire **HAL**, est destinée au dépôt et à la diffusion de documents scientifiques de niveau recherche, publiés ou non, émanant des établissements d'enseignement et de recherche français ou étrangers, des laboratoires publics ou privés.



Monitoring mechanical stimulation for optimal tendon tissue engineering: a mechanical and biological multiscale study

Journal:	<i>Journal of Biomedical Materials Research: Part A</i>
Manuscript ID	JBMR-A-20-0611
Wiley - Manuscript type:	Original Article
Date Submitted by the Author:	07-Sep-2020
Complete List of Authors:	Garcia, Alejandro; Sorbonne Université, mechanical engineering Perot, Jean-baptiste; Compiegne University of Technology, Biomechanics and Bioengineering Beldjilali-Labro, Megane; Compiegne University of Technology, Biomechanics and Bioengineering Dermigny, Quentin; Compiegne University of Technology, Biomechanics and Bioengineering Le Ricousse, Sophie; Université de Picardie Jules Verne, EA7516 CHIMERE Legallais, Cécile; Compiegne University of Technology, Biomechanics and Bioengineering Naudot, Marie; Université de Picardie Jules Verne, EA7516 CHIMERE Bedoui, Fahmi; Sorbonne Université, mechanical engineering
Keywords:	Electrospinning, Mechanical stimulation, Stem cells, Tissue engineering, tendon

SCHOLARONE™
Manuscripts

1 **Monitoring mechanical stimulation for optimal tendon tissue engineering: a** 2 **mechanical and biological multiscale study**

3
4 Garcia Garcia A.¹, Perot JB.¹, Beldjilali-Labro M.¹, Dermigny Q.¹, Naudot M.², Le Ricousse
5 S.², Legallais C.¹, Bedoui F.^{3,*}

6 ¹ CNRS, UMR 7338 Laboratory of Biomechanics and Bioengineering, Sorbonne Universités,
7 Université de Technologie de Compiègne, 60200 Compiègne, France

8 ² EA4666-LNPC-Immunologie Therapie Cellulaire Hématologie Cancers, CURS, Hôpital
9 Sud Avenue René Laennec, 80054 Salouel, France

10 ³ FRE CNRS 2012 Roberval Laboratory for Mechanics, Sorbonne Universités, Université de
11 Technologie de Compiègne, 60200 Compiègne, France

12 * Correspondence: fahmi.bedoui@utc.fr; Tel.: +33- 3 44 23 45 28

14 **ABSTRACT**

15 To understand the effect of mechanical stimulation on cell response, bone marrow stromal
16 cells were cultured on electrospun scaffolds under two distinct mechanical conditions (static
17 and dynamic). Comparison between initial and final cell construct mechanical and biological
18 properties were conducted over 14 days for both culturing conditions. As a result,
19 mechanically stimulated constructs, in contrast to their static counterparts, showed evident
20 mechanical-induced cell orientation, a high amount of aligned collagen along with an
21 abundance of tenomodulin differentiation phenotype. Cell orientation and high collagen
22 production and orientation lead to enhanced storage modulus observed under dynamic
23 stimulation. The increase in tenomodulin under dynamic conditions provided clues on the
24 importance of mechanical stimulation to induce tendon-like phenotype production.
25 Altogether, mechanical stimulation lead to (i) morphological orientation were static cultured
26 constructs presents random morphology, (ii) more pronounced elastic behavior with a
27 limited viscous contribution in the global mechanical response. Such a correlation could help
28 in further studies to use mechanical stimulation as chemical-free cell guidance in tissue
29 engineering development.

1
2
3 30 Key words: Electrospinning, Mechanical stimulation, Stem cells, Tissue engineering, tendon
4
5
6 31

7
8 32 **Introduction**
9

10 33 The main objective of tendon tissue engineering is to design and produce a cell-construct
11 34 that will help to regenerate damaged tissue or mimic it for comprehensive in vitro studies.

12
13
14 35 To achieve this goal, different groups have searched in recent years for the most efficient
15 36 cells, the right materials, and the appropriate chemical or mechanical environment(1,2).

16
17 37 Although the holy grail is still a long way off, most studies have clearly demonstrated the
18 38 advantages of reproducing the mechanical environment in order to guide the cell-scaffold
19 39 constructs towards tendon repair(2).
20
21
22

23 40 Biomimetic analysis can be considered as essential to guide choices in advanced tissue
24 41 engineering. Native tendon is made of an anisotropic and viscoelastic material capable of
25 42 resisting high tensile forces. Tendon cells, mainly tenocytes, are rather scarce, and are
26 43 responsible for synthesising extracellular matrix, which is mainly composed of type I
27 44 collagen with a highly organised structure.
28
29
30
31
32

33 45 As primary tenocytes are rather difficult to collect, bone marrow stromal cells (BMSC) are
34 46 the most widely used stem cells for tendon tissue engineering, among other stem or
35 47 progenitor cells, as they have the potential for self-renewal, clonogenicity, and multi-lineage
36 48 differentiation, including tenogenicity(3,4).
37
38
39
40

41 49 Regarding the scaffold issue, electrospinning has been used for several years to tailor an
42 50 environment for cell development and differentiation similar to that of extracellular matrix,
43 51 but with different fibre sizes, porosity, elasticity and mechanical properties for tendon tissue
44 52 engineering(5). Recently, Lee et al. showed that small, nano-scale random fibres provided a
45 53 cell environment similar to that found in the inflammatory phase of the tendon healing
46 54 process, promoting the synthesis of the extracellular matrix (ECM) and cell proliferation,
47 55 while larger aligned fibres mimicked the normal structure of collagen in tendon, maintaining
48 56 the tendon cell phenotype(6).
49
50
51
52
53
54
55

56 57 Mechanical stimulation is another key environmental factor for reproducing in vivo
57 58 conditions. Physiotherapists recommend periodic stretching in training to heal defects or to
58
59
60

1
2
3 59 improve capacity(7–10). In vitro, some studies have stated that proper stimuli applied to
4
5 60 biohybrid scaffolds could act on cell proliferation, differentiation or function, following
6
7 61 mechanotransduction pathways(11–13). While different stimuli have been tested with a
8
9 62 wide range of amplitudes, frequencies and time, it should be noted that little is known
10
11 63 about how mechanical stress may affect both cell and material responses throughout the
12
13 64 tissue engineering process(14). In addition, the parameters assessing the evolution over
14
15 65 time of the cell-constructs' mechanical properties are not always relevant. Elastic modulus,
16
17 66 stiffness and ultimate tensile strength seem to be accepted as the standard in the field(4).
18
19 67 However, native tendon is a viscoelastic material, combining viscous liquid-like, and solid-
20
21 68 like behaviour. While the notion of viscoelasticity includes time dependency, meaning that
22
23 69 the mechanical response depends on the deformation rate (ϵ), tendon tissue engineered
24
25 70 constructs tend to be characterised by quasi-static mechanical tests as ranges of strain that
26
27 71 do not reproduce physiological conditions. These parameters emphasise on the elastic
28
29 72 properties of the material, at a supra-physiological level and with a limited real application.
30
31 73 Measured at the beginning and at the end of each experiment, a day-to-day evolution of the
32
33 74 mechanical properties of different materials remains utopic.

33
34 75 The objective of this study was to establish a time resolving monitoring approach of the
35
36 76 mechanical properties of cell construct under different culturing conditions. Thus, the
37
38 77 precise and relevant change in the measured mechanical properties could be used to
39
40 78 interpret the cells' responses in close correlation to the chosen biological indicators. Such
41
42 79 correlation could help in further studies to use mechanical stimulation as chemical-free cell
43
44 80 guidance in tissue engineering development.

45
46 81 In order to better understand this inter-dependency between mechanical stimulations and
47
48 82 biohybrid scaffold responses, we performed static and dynamic cultures of rat BMSCs on
49
50 83 dedicated random electrospun PCL scaffolds using bioreactors (T6 CellScale and Bose
51
52 84 Biodynamic 5100). The mechanical behaviour under a pseudo-physiological strain and
53
54 85 cellular activity of the cell-constructs during the stimulation period were recorded and
55
56 86 analysed for 12 days, then compared with those obtained under static conditions. At the
57
58 87 biological level, we focused on cell proliferation, differentiation towards tendon lineage (in
59
60 88 the absence of specific differentiation factors) and organisation of the neo-synthesized ECM.

1
2
3 89 At the mechanical level, we followed up the changes in both the viscous and elastic
4
5 90 properties of the pure and cell-seeded scaffolds. Therefore, we propose to evaluate
6
7 91 different mechanical markers of both elasticity and viscoelasticity such as energy
8
9 92 dissipation, damping factor ($\tan \delta$), storage modulus (E') and loss modulus (E''), already used
10
11 93 in the mechanobiology field to analyse the performance of native tendons.

13 94 **Materials and Methods**

16 95 • **Electrospun scaffold preparation and characterisation**

18 96 Poly(ϵ -caprolactone) (PCL, MW=80kg.mol⁻¹ Sigma Aldrich, United States) was dissolved in
19
20 97 dichloromethane (DCM, Sigma-Aldrich)/*N,N*-dimethylformamide (DMF, ReagentPlus® Sigma-
21
22 98 Aldrich, USA) (80/20 v/v) for 24h to make an electrospinning solution at 10 wt %. Once
23
24 99 dissolved, the solution was poured into a 10 ml glass syringe. Scaffold fabrication was
25
26 100 performed over a rotating collector for 3H (distance 15 cm, flow rate 0.017ml/min, needle
27
28 101 diameter 18G, voltage 15kV). In order to evaluate the morphology and mechanical
29
30 102 properties of the PCL scaffolds, scanning electron microscopy and tensile testing were
31
32 103 carried out retrospectively.

34 104 The morphology of the electrospun scaffolds was observed using scanning electron
35
36 105 microscopy (Philips XL30 ESEM-FEG). Electrospun mats were cleaned with ethanol and gold-
37
38 106 coated prior to observation. To analyse the diameter of the electrospun 10 wt % PCL fibres,
39
40 107 ImageJ software was used. After setting up the scale, a line was drawn manually across the
41
42 108 diameter of randomly-selected fibres (n=50) from 3 different SEM micrographs. The degree
43
44 109 of isotropy in two samples from three scaffolds (n=6) was analysed using Mountain™
45
46 110 software. The main directions of the fibres were analysed using the Fourier Transform
47
48 111 method.

49 112 The scaffold modulus for dry and wet scaffolds was quantified using uniaxial tensile testing.
50
51 113 Three samples for each scaffold (n=3) were shaped into a strip measuring 1.0 cm x 3.0 cm.
52
53 114 For wet samples, the scaffolds were immersed in ethanol 70% (Sigma-Aldrich, USA) for 45
54
55 115 min then washed three times with PBS 7.4 (phosphate buffered saline, Gibco Invitrogen,
56
57 116 USA). The thickness was evaluated using a precision dial thickness gauge (Mitutoyo
58
59 117 Corporation, Japan). The samples were secured within the metallic grips of the tensile tester

1
2
3 118 (Bose Electroforce 3200, TA, USA) and elongation at 0.1 mm s^{-1} was performed with a
4
5 119 working load of 22N. The applied force was measured each second and the modulus
6
7 120 obtained from the slope of the linear region.
8
9

10 121 • **Cell harvesting and culture**

11 122 Bone marrow stromal cells (BMSCs) were isolated from rat bone marrow thanks to their
12 123 short-time adherence to plastic, in accordance with previously described protocols(15).
13 124 Briefly, 6-week-old male Sprague Dawley rats (n=4) were sacrificed, and both right and left
14 125 femurs were aseptically removed and washed 3 times with 1x PBS 7.4 (phosphate buffered
15 126 saline, Gibco Invitrogen, USA). Next, bone marrow was flushed out using α -MEM culture
16 127 medium (PAN BIOTECH, Germany) supplemented with 10% foetal bovine serum (FBS, Gibco
17 128 Invitrogen, USA), 1% penicillin-streptomycin (Gibco Invitrogen, USA) and 1% amphotericin B
18 129 (PAN BIOTECH, Germany). The released cells were then collected into 6-well dishes (BD
19 130 Falcon™, USA). After 24h, non-adherent cells were carefully discarded and adherent cells
20 131 were cultured with fresh α -MEM for 6-7 days, the time needed for BMSC colonies to reach
21 132 confluence. The cell culture media were replaced every 3 days. When the culture dishes
22 133 started to approach confluence, the cells were detached and serially subcultured. The cells
23 134 at the third passage (P3) were used for the cell seeding experiments. Experimental
24 135 procedures involving animals were carried out on euthanised animals within the approved
25 136 structure (E60 159 01). Both the procedures and the treatment of the animals complied
26 137 with the principles and guidelines of the French legislation on animal welfare (No. 2013-118)
27 138 and the Directive if the European Communities (2010/63/EU).
28
29
30
31
32
33
34
35
36
37
38
39
40
41
42

43 139 Electrospun mats were cut into strips measuring 40 x 12.5 mm or 35 x 9 mm as shown in
44 140 **Supplementary Table ST2**, disinfected with ethanol 70% (Sigma-Aldrich, USA) for 45 min,
45 141 and then washed three times with PBS for 10 min. Disinfected scaffolds were soaked in
46 142 fresh α -MEM for 48h before seeding the cells. After that, the media was discarded and each
47 143 scaffold was plated with a density of $6 \times 10^4 \text{ cells cm}^{-2}$.
48
49
50
51
52

53 144 • **Mechanical stimulation**

54 145 After two days of static culture, each construct was placed in a bioreactor for mechanical
55 146 stimulation or in well dishes for static culture. Mechanically-stimulated cell constructs were
56 147 stretched twice a day at 5% strain for 1h at 1Hz with 11h of rest between each cycle for 5 or
57
58
59
60

1
2
3 148 12 days (considered as 1 or 2 weeks of culture time respectively). For this purpose, two
4
5 149 different bioreactors were used: (1) the MechanoCulture T6 Mechanical Stimulation System
6
7 150 (CellScale Biomaterials Testing, Waterloo, ON, Canada), consisting of an actuator and screw-
8
9 151 driven clamp grips mounted inside a cell culture chamber capable of applying uniaxial
10
11 152 stretching to 6 parallel samples, was chosen for the biological assays. Cell culture media
12
13 153 were replaced every 5 days, and (2) the Bose Biodynamic 5100 (TA Electroforce®, USA),
14
15 154 consisting of a cell culture chamber connected to a flow pump in which one sample was
16
17 155 attached thanks to a system of rods and clamps. One rod was attached to a step motor
18
19 156 making it possible to apply uniaxial displacement. The other rod was connected to a force
20
21 157 transducer of 22N making it possible to constantly monitor the force applied to each
22
23 158 displacement. Cell culture media circulated continuously through the flow pump connected
24
25 159 to a reservoir of 500 mL, making it possible to maintain the culture for up to two weeks. This
26
27 160 system was chosen for biomechanical evaluation. For static culture, each construct was
28
29 161 cultured for 5 or 12 days without tension and the cell culture media were replaced every 3
30
31 162 days.

31 163 **Biological and mechanical evaluation of cell-constructs**

32
33 164 To investigate the effects of dynamic culture on cell activity, seeded PCL 10-wt % scaffolds
34
35 165 were secured in the grips of the T6 CellScale bioreactor after two days of static culture and
36
37 166 cultured for 5 or 12 days under dynamic culture conditions (5% strain for 1h at 1Hz with 11h
38
39 167 of rest). After this time, the cell-constructs were removed for biological analyses.

40
41 168 Total deoxyribonucleic acid (DNA) and collagen from each sample were extracted at 5 or 12
42
43 169 days of static or dynamic culture with the reagent, Trizol (TRI Reagent®, Sigma-Aldrich, USA)
44
45 170 according to the manufacturer's protocol. Briefly, once lysed by the action of 1ml of Trizol,
46
47 171 chloroform (Sigma-Aldrich, USA) was added to obtain a colourless upper aqueous phase
48
49 172 with RNA, an interphase with DNA, and a lower red phenol-chloroform phase with proteins.
50
51 173 DNA was then isolated and quantified using NanoDrop ND-1000 (Thermo Scientific, USA).
52
53 174 Proteins were isolated and hydrolysed in 6N HCl (Sigma-Aldrich, USA), and total
54
55 175 hydroxyproline content was determined using hydroxyproline assay (Hydroxyproline Assay
56
57 176 Kit, Sigma-Aldrich, USA)(16). Hydroxyproline content was related to the collagen
58
59 177 content(17).
60

1
2
3 178 After 5 or 12 days of static or dynamic culture, cells-constructs were fixed in a solution of 4%
4 179 (w/v) paraformaldehyde solution (PAF, Agar Scientific, United Kingdom) in PBS for 15 min
5 180 then rinsed three times with PBS 7.4. After 10 min of permeabilization in a solution of PBS-
6 181 Triton X-100 0.5% (v/v) (VWR, United Kingdom), cell-constructs were blocked at 4°C
7 182 overnight with a solution of 1% (w/v) BSA (Sigma-Aldrich, USA). The morphology of the
8 183 rBMSCs under static or dynamic culture was assessed using rhodamine phalloidin
9 184 (Invitrogen, USA) to selectively stain the F-actin. For immunofluorescence staining, cell-
10 185 constructs were treated with mouse primary antibodies anti-rat collagen type I (COL1,
11 186 1:100, Abcam, United Kingdom) or to anti-rat tenomodulin (TNMD, 1:200, Abcam, United
12 187 Kingdom) overnight at 4°C. After incubating overnight at 4°C with secondary fluorescent
13 188 antibodies donkey anti-mouse 488 (Invitrogen, USA). Hoechst 33342 (Sigma-Aldrich, USA)
14 189 was added as counterstaining for cell nuclei. Z-stacks were then acquired on an Inverted
15 190 ZEISS 710 confocal microscope (Zeiss, Germany).

16 191 To investigate the effects of dynamic culture on the evolution of the mechanical properties
17 192 of the cell-constructs, seeded scaffolds or scaffolds without cells were mounted in the Bose
18 193 Biodynamic 5100 for 12 days under mechanical stimulation. Bose Biodynamic 5100 consists
19 194 of one culture chamber with two rods, one connected to a motor and the other to a force
20 195 transducer of 22N. The entire system is placed in an incubator making it possible to control
21 196 the temperature and CO₂ at 37°C and 5% respectively. Cell culture media circulated
22 197 continuously thanks to a system of peristaltic pumps connected to the cell chamber. The
23 198 bioreactor makes it possible to apply defined cyclic (sinusoidal) strain to the cell-seeded or
24 199 empty scaffolds, and to concomitantly record the resulting stress. Either stress (σ) or strain (ϵ)
25 200 could be set up as the driving parameter. We decided to set deformation, 5% cyclic
26 201 sinusoidal strain as the control parameter. We recorded the resulting force at 20 points per
27 202 second, corresponding to 20 points per sinus, during the 12 days of dynamic culture.

$$28 \text{ 203 } \quad \textit{Strain } \epsilon = \epsilon_0 \sin \omega t \quad (1)$$

$$29 \text{ 204 } \quad \textit{Stress } \sigma = \sigma_0 \sin (\omega t - \delta) \quad (2)$$

30 205 Where ϵ_0 and σ_0 are the initial strain and stress respectively, and ω and δ are the frequency
31 206 and dephasing angle between stress and strain respectively. Plotting together stress vs
32 207 strain, we were able to calculate the relative dissipation energy by calculating the surface

208 between the curves in each sinus. Because sinusoidal stress was applied, we also
209 determined the storage modulus (E'), loss modulus (E''), complex modulus (E^*) and $\tan \delta$.
210 All equations are indicated below:

$$E' = \frac{\sigma_0}{\varepsilon_0} \cos(\delta) \quad (3)$$

$$E'' = \frac{\sigma_0}{\varepsilon_0} \sin(\delta) \quad (4)$$

$$E^* = \sqrt{E'^2 + E''^2} \quad (5)$$

$$\tan(\delta) = \frac{E''}{E'} \quad (6)$$

215 For analysis, each 1h cycle, consisting of 3600 sinuses, was divided into six intervals of 600
216 sinus and the results are given as an arithmetic average. After the first analysis, we decided
217 to represent the results from 1200 to 3600 sinus of each cycle, where a closed loop region
218 was found. For statically-cultured cell-constructs and controls, each sample was placed on
219 the bioreactor and, once secured between the rods, one cycle of 3600 sinus was set at a
220 given time (7 and 14 days) to compare in the same way as the dynamic conditions. For the
221 control without cells, scaffolds were subjected to the same parameters as the cell-
222 constructs, including disinfection and incubation with cell culture media.

223 **Statistical analysis**

224 At least 6 independent experiments, except for the biomechanical analysis ($n=3$) carried out
225 on the Bose Biodynamic 5100, were performed. Each result (mechanical properties as
226 damping factor, loss and storage modulus) represents an arithmetic average the different
227 analyzed tests. Data are therefore presented as an average along with the appropriate mean
228 standard deviation. The significance of the results was tested by analysing the variance
229 (ANOVA) with Turkey's post hoc test in the case of multiple comparisons.

230 On behalf of the authors, we declare, that all the methods were carried out in accordance
231 with relevant guidelines and regulations. In addition all experimental protocols were
232 approved by our institution (Sorbonne Université Alliance, Université de Technologie de
233 Compiègne) committees.

234 Results

235 • PCL scaffold synthesis and characterisation

236 Scaffolds were prepared using electrospinning laboratory made setup (**Fig 1**). The prepared
237 scaffolds were meant to be used for cell culture under different conditions; static and
238 dynamic culturing as presented schematically in figure 2 (**Fig 2**). Electrospinning PCL into a
239 DCM/DMF 4:1 co-solvent led to the production of a homogenous scaffold without pearls.
240 SEM images showed a final material composed of a dense network of continuous smooth
241 fibres (**Fig 3A**), as found in (18). These fibres presented an average diameter of 0.52 ± 0.25
242 μm . Distribution analyses of the fibres revealed a random conformation (**Fig 3B**).

243 The scaffolds were then characterised following the uniaxial traction test described in the
244 Materials and Methods section. In order to evaluate potential alteration of the mats in an
245 aqueous solution, the scaffolds were analysed in both dry and wet conditions. Stress/strain
246 profiles were similar, showing a “J” zone, characteristic of the nonlinear mechanical
247 response of material, in which we were able to identify three different regions; the toe
248 region (<2% strain), heel region (<8% strain) and linear region (<18% strain) (**Fig 4A**). Both
249 elastic moduli were similar, with 8.05 ± 0.82 MPa for the dry scaffolds and 7.93 ± 2.66 MPa
250 for the wet ones (**Fig 4B**).

252 • Biological outcomes and tendon extracellular matrix deposition

253 The number of cells presented on the constructs was assessed by means of DNA
254 quantification. The amount of DNA was observed in either static or dynamic conditions after
255 2 weeks (**Fig 5#**). Dynamic stimulated cell-constructs appeared to have greater number of
256 cells compared to static cultures with $4.1 \pm 1.3 \times 10^6$ vs $2.91 \pm 0.8 \times 10^6$ respectively, after 2
257 weeks of culture, although the difference was not statistically significant.

258 In order to determine the effect of the mechanical stretching on ECM neo-synthesis,
259 hydroxyproline was measured (**Fig 5§**). Hydroxyproline concentration is related to fibrillar
260 collagen and comprises around 13.5% of the collagen(19). It could be detected in all the
261 culture conditions. After a week of culture, no difference in collagen production was
262 observed between the static or dynamic conditions. After two weeks, a significant increase
263 in collagen synthesis under dynamic stretching was noted, with 18.8 ± 2.6 μg vs 12.1 ± 1.4

264 μg of hydroxyproline for the static culture. Mechanical stimulation thus induced elevated
265 collagen content in the scaffold, compared to the static culture.

266 To better understand cell organisation, fluorostaining of the actin cytoskeleton was
267 performed (**Fig 5***). Cells cultured in the absence of mechanical stimulation presented a
268 random morphology on the scaffold. This behaviour did not evolve with culture time, with
269 the same observations at 1 or 2 weeks (**Fig 5* A-D**). On the contrary, when submitted to
270 mechanical stimulation, cells presented an elongated shape and appeared aligned with the
271 stretching direction. This effect seemed more pronounced after two weeks of stimulation,
272 with thinner elongated cells at the surface of the material (**Fig 5* D**).

273 To determine the possible differentiation of BMSCs towards tendon lineage under both
274 static and dynamic culture conditions, immunofluorescence staining of type 1 collagen, the
275 main constituent of tendon ECM, and tenomodulin, a tendon specific marker, was
276 performed at different time points. Type-1 collagen was found in both conditions at 1 or 2
277 weeks of culture (**Fig 5* E-H**). After 1 week of culture, type-1 collagen structures were
278 aligned with the stretching under dynamic conditions (**Fig 5* F**), while in static culture they
279 were present in a random manner (**Fig 5* E**). After 2 weeks of culture, the same trend was
280 confirmed. Collagen fibres seemed to be more abundant compared with the first week of
281 culture (**Fig 5* G, H**). While there were some clusters of aligned collagen on the static
282 culture (**Fig 5* G**), under the effect of mechanical stimulation, the collagen was highly
283 organised, with collagen fibres aligned towards the stretching axis.

284 Immunofluorescence staining revealed the presence of tenomodulin on both culture
285 conditions. In the same manner as collagen fibres, an alignment was observed when the
286 cell-constructs were mechanically stretched (**Fig 5* I-L**). After one week of culture,
287 tenomodulin appeared to be clearly aligned under dynamic conditions (**Fig 5* J**) compared
288 to the static culture (**Fig 5* I**). This effect was more difficult to visualise after two weeks due
289 to the total distribution of tenomodulin and the high cell density (**Fig 5* K, L**).

290

- 291 • **Mechanical stimulation and biomechanical evaluation of cell construct**

292 Initially, static tests were conducted on dry and wet scaffolds. Those tests help deriving
293 elastic modulus (E) by plotting the slope of the stress vs strain curve, corresponding to the
294 linear zone of our material as shown in figure 4 (**Figure 4**), due to the non-linearity at the

1
2
3 295 initial part of the curve. Dynamic testing were, however conducted at 5% dynamic strain,
4
5 296 which means that the dynamic strain was imposed within the non-linear regime of the
6
7 297 stress-strain curve.
8

9
10 298 After 2 days of static culture, the cell-construct or the control scaffolds were fixed inside the
11
12 299 bioreactor chamber and the mechanical test was launched. Both signal force and
13
14 300 displacement were recorded over time and found to be smooth, without any background
15
16 301 noise, making it possible to monitor mechanical (elastic and viscoelastic) properties (**Fig 6A**).

17
18 302 The relative dissipation energy or hysteresis can be calculated by calculating the surface
19
20 303 area between the curves, along with the damping factor (**Fig 6A**). All the relevant
21
22 304 parameters were extracted following the equations described previously and presented in
23
24 305 **Fig 7**, to follow the tissue response continuously instantaneously and after two weeks of
25
26 306 culture.

27
28 307 Initially (i.e. on day 2), in terms of viscous ($\tan \delta$, dissipated energy and E'') and elastic (E')
29
30 308 properties, along with the complex modulus (E^*), no **significant differences** were found
31
32 309 between the different parameters for the different culture conditions with or without cells,
33
34 310 however, slight trends can be drawn between the different conditions. For $\tan \delta$, similar
35
36 311 values were found for each condition in both cell constructs and controls with 0.08 ± 0.01 vs
37
38 312 0.12 ± 0.03 in static conditions and 0.09 ± 0.01 vs 0.09 ± 0.03 in dynamic ones. For the
39
40 313 dissipated energy (hysteresis), cell-constructs seemed to present lower values than controls,
41
42 314 with 0.64 ± 0.35 vs 0.92 ± 0.14 in static conditions and 0.90 ± 0.11 vs 1.47 ± 0.57 in dynamic
43
44 315 ones (**Fig 7**). For E'' , another parameter related to viscosity, the same trend was found, with
45
46 316 lower values for cell-constructs (0.30 ± 0.16 MPa & 0.37 ± 0.13 MPa) in both static and
47
48 317 dynamic conditions, compared to controls (0.42 ± 0.07 MPa & 0.59 ± 0.14 MPa). In terms of
49
50 318 elastic properties, the storage modulus (E') appeared higher for the dynamic control with
51
52 319 6.63 ± 0.89 MPa. E^* followed the same trends as E' , with the highest value found for
53
54 320 dynamic control (6.68 ± 0.87 MPa).

54
55 321 After 14 days of culture, the results showed a slight increase in $\tan \delta$, dissipated energy and
56
57 322 E'' for cell-constructs, both static and dynamically cultured (**Fig 7**), compared to both static
58
59 323 and dynamic controls. For E' and E^* , the same trend was found after 14 days of culture, with
60

1
2
3 324 values for statically cultured cell-constructs of 4.24 ± 0.78 MPa and 0.44 ± 0.08 MPa
4
5 325 respectively and 5.04 ± 0.11 MPa and 0.49 ± 0.02 MPa for cell-constructs under dynamic
6
7 326 stimulation.

8
9 327 To better determine the effects of mechanical stimulation and cell culture on different
10
11 328 groups, we decided to analyse the variation (V%) in the mechanical parameters (P) between
12
13 329 the first cycle of day 2 (i.e. the first day of mechanical stimulation) and the last cycle of day
14
15 330 14 (i.e. the last day of culture) (**Fig 8**). $V\% = 100 * (P_{d14} - P_{d2}) / P_{d2}$.

16
17 331 Although not statistically significant, some trends are present in each of the mechanical
18
19 332 properties analysed. In the absence of cells, all mechanical parameters presented lower
20
21 333 percentages than those obtained in cell-constructs (**Figure 8**). $\tan(\delta)$ presented a slight
22
23 334 increase for static controls ($4 \pm 7\%$) and decreased for dynamic ones ($-3 \pm 6\%$). For
24
25 335 dissipated energy, controls presented a decrease of $-4 \pm 17\%$ and $-10 \pm 2\%$ for static and
26
27 336 dynamic conditions respectively. E'' presented the same trend as dissipated energy, with the
28
29 337 highest decrease obtained for static conditions (-25 ± 4) compared to dynamic ones ($-9 \pm$
30
31 338 6%). The elastic parameter (E') appeared to decrease particularly for the static control ($-20 \pm$
32
33 339 9%), compared to a slight reduction for the dynamic control ($-6 \pm 0.1\%$). E^* followed the
34
35 340 same trends as E' , with the highest decrease found with the static control with $-20 \pm 9\%$ vs -
36
37 341 $6 \pm 0.2\%$ for the dynamic control.

38
39 342 In the presence of cells, $\tan \delta$ seemed to increase in both static and dynamic cultures, with
40
41 343 an enhancement of $22 \pm 16\%$ and $16 \pm 5\%$ respectively. Dissipated energy presented a
42
43 344 similar trend with enhancement of $25 \pm 7\%$ and $14 \pm 9\%$ for static and dynamic culture of
44
45 345 cell-constructs, respectively. In terms of E'' , cell-constructs presented an increase of $45 \pm 5\%$
46
47 346 for static and $31 \pm 19\%$ for dynamically-cultured cell-constructs. For E' , dynamically-cultured
48
49 347 cell-constructs presented the highest increase, with $16 \pm 20\%$, while for static cultures a
50
51 348 slight increase of $7 \pm 6\%$ was found. Regarding E^* , the same trends appeared as for E' , with
52
53 349 the highest increase for dynamic conditions ($16 \pm 20\%$).

54
55 350 Static control appeared to have the lowest values for E' , E'' and E^* , followed by dynamic
56
57 351 control. On the other hand, both cell-constructs (dynamic or static cultured) presented the

1
2
3 352 highest enhancement of mechanical properties over time, with higher viscosity for static
4
5 353 conditions and higher elasticity for dynamic ones
6
7

8 354 **Discussion**

9
10 355 Our scientific goal was to understand any correlation between the changes on the
11
12 356 mechanical properties of the biohybrid scaffold and the activity of the seeded BMSCs, in
13
14 357 association with the production and arrangement of the newly-formed ECM produced by
15
16 358 cells. To the best of our knowledge, this analysis, which requested an adequate cell culture
17
18 359 protocol, has not yet been investigated. Therefore, we first needed to confirm the role of
19
20 360 mechanical stimulation on BMSC differentiation towards tendon lineage when cultured on
21
22 361 adapted scaffolds.
23

24 362 In this study, we proposed to follow the cell-constructs' mechanical properties with a set of
25
26 363 relevant parameters (E' , E'' and $\tan \delta$) throughout the entire dynamic stimulation and key
27
28 364 parameters of cell activity as proliferation, orientation differentiation. Our experiment,
29
30 365 generating 5% of strain at 1Hz, represents a dynamic testing involving continuous repeated
31
32 366 sine strain simulating physiological activities for tendons(20).
33

34 367 Our first concern was thus to develop a biomaterial suitable for this approach.
35
36 368 Electrospinning has been widely used in the development of materials mimicking the fibrous
37
38 369 nature of the tendon extracellular matrix(21). While our PCL scaffold presented an elastic
39
40 370 modulus of 8.05 ± 0.82 MPa (**Fig 3**), which is still a long way from native tendon(22), the
41
42 371 stress-strain curve revealed three regions similar to those found in tendons(4). Taking into
43
44 372 account this stress-strain response, and comparing them with the mechanical behaviour of
45
46 373 tendon, we decided to apply a cyclic sinusoidal strain of 5% (0-5%) corresponding to the
47
48 374 heel region of both tendon and our electrospun scaffold. This was intended to calculate the
49
50 375 viscoelastic behaviour of our cell-constructs when submitted to cyclic stretching with
51
52 376 repeated stretching cycles and strain rates within a low range. The effect of this mechanical
53
54 377 protocol was analysed for cell behaviour, mechanical changes over time and the correlation
55
56 378 between both variables.

57 379 (1) Cell behaviour over mechanical stimulation
58
59
60

1
2
3 380 Regarding the cell behaviour, after one week of culture, there was no difference in terms of
4
5 381 proliferation between static and dynamic conditions (**Fig 5#**). After two weeks, the number
6
7 382 of cells was found to have tripled for the static culture and even quadrupled for cells
8
9 383 submitted to dynamic stretching. We can thus conclude that the mechanical stimulation
10
11 384 enhanced the proliferative ability of BMSCs, inducing an increase in cell proliferation in
12
13 385 response to mechanical load. This result is consistent with other experiments conducted
14
15 386 with BMSCs, where more cells were found after 2 weeks of culture compared to shorter
16
17 387 culture times under 5% of stretching(23). Other studies have shown similar results with
18
19 388 fibroblasts(24) and TDSCs(25). While an increase in cell proliferation is found as a response
20
21 389 to mechanical stimulation, the mechanisms involved in this mechano-response still need to
22
23 390 be clarified(26).

24
25 391 When stimulated, BMSCs presented an elongated morphology aligned with the stretching
26
27 392 direction (**Fig 5* B,D**), while cells cultured under static conditions were randomly organised
28
29 393 on the scaffold (**Fig 5* A,C**). Similar behaviour was found in another study that analysed the
30
31 394 impact of mechanical stimulation on cell alignment when cultured on randomly-oriented
32
33 395 scaffolds in the same range of nanofiber size(27).

34
35 396 Regarding collagen synthesis, the cell-constructs showed continuous production over time,
36
37 397 with more collagen found after 2 weeks of culture for each condition (**Fig 5§**). After two
38
39 398 weeks of culture, more collagen was found on cell-constructs subjected to mechanical
40
41 399 stretching, in agreement with several other studies(28–30). This effect has been shown
42
43 400 consistently in in vivo studies carried out on tendons where an increase in collagen synthesis
44
45 401 was observed as a part of the tendon adaptation response to continuous mechanical
46
47 402 loading(31).

48
49 403 Analysis of the ECM produced by cells in both static and dynamic cultures was also
50
51 404 performed by immunofluorescence staining of type I collagen and tenomodulin (**Fig 5***).
52
53 405 Collagen I is the most abundant collagen in tendons, and tenomodulin is a late tendon
54
55 406 differentiation marker, and a key glycoprotein for the mature state of tendons(32,33). Both
56
57 407 were more abundant under mechanical stimulation when compared to static culture
58
59 408 samples. Furthermore, they appeared to be arranged in the stretching direction. Taken
60
409 together, these data with cell alignment achieved in dynamic conditions, revealed a tendon-

1
2
3 410 like phenotype of BMSCs under dynamic culture conditions, similar to native tendon
4
5 411 arrangement(34).
6

7
8 412 (2) Mechanical stimulation; impact of the culturing conditions.
9

10 413 Concerning the evolution of the biomechanical behaviour and to avoid the noise, we
11 414 decided to analyse and represent the V% of the targeted parameters variations as
12 415 described before with the equations, from the 1200 to 3600 sinus where a neat loop was
13 416 observed, similar to the mechanical behaviour observed in tendons(35). For both static and
14 417 dynamic controls, E' , E'' and $\tan \delta$ seem to present a reduction while for cell constructs
15 418 those parameters seem to increase over time (**Fig 8**), which maybe result of cellular
16 419 behaviour.
17

18 420 The elastic modulus E' considers the elastic properties both from the material and for cells.
19 421 The increase over time could be explained as the result of newly deposited type I collagen
20 422 fibres. Type I collagen is effectively an important stress-bearing component of connective
21 423 tissues. It is secreted by cells and hierarchically assembled into fibrils from a packaging of
22 424 collagen molecules, embedded in a soft matter formed of water and proteoglycans. This
23 425 organisation gives the collagen structure enough rigidity to be considered an elastic
24 426 beam(36). In addition, the aligned orientation adopted by collagen fibres (Fig 5*) through
25 427 the stretching direction could explain the higher E' percentage (16%) for dynamically-
26 428 cultured cell-constructs compared to static culture (7%), as aligned collagen fibres are better
27 429 suited up to supporting tensile stress(37).
28

29 430 The loss modulus (E'') takes into account the viscous behaviour, therefore its energy
30 431 dissipation behaviour and confirmed our previous results. As seen before, when initial and
31 432 last values were compared (**Fig 8**), the controls without cells presented a reduction in E''
32 433 with -25% for static and -9% for dynamic controls.
33

34 434 The cell-constructs showed an increase of E'' for both static and dynamic conditions.
35 435 However, this increase seemed to be higher for static conditions with 45% increase,
36 436 compared with 31% for dynamic cultures. Taken together, these results consistently
37 437 demonstrated that cell-constructs, presented increased viscosity over time, compared to
38 438 nude biomaterials. Finally, dynamic cultures exhibited a greater increase in the elastic
39 439 properties of the cell-constructs, with a lesser gain in viscous properties, while the static
40

1
2
3 440 cultures had a greater influence on the viscous properties, with a lower increase in
4
5 441 elasticity.

6
7 442 This effect may be explained by the effect of the alignment of the extracellular matrix,
8
9 443 particularly the collagen fibres, which align through the tensile axis, resulting in an increase
10
11 444 in the elastic properties of the cell-constructs exposed to dynamic culture conditions (**Fig**
12
13 445 **5***).

14 446 Others viscous related parameters as $\tan \delta$ seem to be in accordance with these results. The
15
16 447 value of $\tan \delta$ is an indicator of how efficiently the material absorbs and dissipates energy
17
18 448 due to fiber-cells rearrangements and internal friction. When we compared its evolution
19
20 449 over time (**Fig 8**), both controls presented the lowest values.

21 450 Cell-constructs, in both static and dynamic cultures, presented an enhanced $\tan \delta$ of 22%
22
23 451 and 16% respectively, compared to cell-free control scaffolds (**Fig 8**). Because $\tan \delta$
24
25 452 represents the ratio of Loss over storage modulus, the highest values of $\tan \delta$ were related
26
27 453 to a higher damping factor. In a rabbit Achilles tendon regeneration model, Nagasawa et al.
28
29 454 found higher values of $\tan \delta$ for regenerated tendons after surgery compared to
30
31 455 controls(33). This increase was explained as the result of the neosynthesis of collagen fibres.
32
33 456 As this "new" fibre presented a lower amount of mature cross-linking, collagen mobility was
34
35 457 increased within the tissue, resulting in more energy dissipation. This may explain the
36
37 458 increase in $\tan \delta$ in our cell-constructs, where cells produced collagen, compared to controls
38
39 459 without cells. In addition, the random organisation of collagen fibres for static conditions
40
41 460 may explain the greater $\tan \delta$ percentages. These results are in accordance with others
42
43 461 mechanical parameters studied here (Supplementary data) as energy dissipation and E^* .

44 462 Correlating both the biological and mechanical results (**Fig 9**), it seems that mechanical
45
46 463 stimulation has a positive effect on cell proliferation and collagen synthesis, which was
47
48 464 greater than static culture conditions. Cell and collagen alignment, together with an increase
49
50 465 in tenomodulin under dynamic culture conditions, provides a better environment for BMSCs
51
52 466 to differentiate towards a tendon-like phenotype. Furthermore, the mechanical properties
53
54 467 of the cell-constructs were enhanced over time compared to the control scaffolds without
55
56 468 cells. This could be explained as a result of the cellular activity, translated into the
57
58 469 production of an ECM. By synthesising collagen, which in tendons and ligaments is
59
60 470 responsible for its mechanical properties, the viscous properties ($\tan \delta$, dissipated

1
2
3 471 energy and E'') were increased in both the static and dynamic cultures. The random nature
4
5 472 of this ECM conferred higher viscous properties for cells cultured under static conditions,
6
7 473 explained as an increase in the mobility of collagen and the associated water molecules
8
9 474 within these random fibres, while dynamically-stimulated cell-constructs presented aligned
10
11 475 collagen fibres towards the direction of the stretching. These aligned fibres could better
12
13 476 retain water molecules, resulting in less mobility compared to random ones. In addition, due
14
15 477 to the elastic nature of the collagen fibres when they are stretched, the alignment may
16
17 478 explain a greater increase in elasticity (E') under mechanical cultivation.

479 **Acknowledgment**

480 This work was carried out and funded in the framework of the Labex MS2T. It was
481 supported by the French Government, through the program "Investments for the future"
482 managed by the National Agency for Research (reference ANR-11-IDEX- 0004-02) and by
483 Région Hauts de France (INTIM project).

484 **Data availability**

485 The data supporting the findings of this study are available from the authors upon
486 reasonable request.

487 **References**

- 488 1. Shearn JT, Kinneberg KRC, Dymont NA, Galloway MT, Kenter K, Wylie C, et al. Tendon
489 Tissue Engineering: Progress, Challenges, and Translation to the Clinic. *J Musculoskelet
490 Neuronal Interact.* 2011 Jun;11(2):163–73.
- 491 2. Butler DL, Juncosa-Melvin N, Boivin GP, Galloway MT, Shearn JT, Gooch C, et al.
492 Functional tissue engineering for tendon repair: A multidisciplinary strategy using
493 mesenchymal stem cells, bioscaffolds, and mechanical stimulation. *J Orthop Res Off
494 Publ Orthop Res Soc.* 2008 Jan;26(1):1–9.
- 495 3. Yin Z, Chen X, Chen JL, Shen WL, Hieu Nguyen TM, Gao L, et al. The regulation of
496 tendon stem cell differentiation by the alignment of nanofibers. *Biomaterials.* 2010
497 Mar;31(8):2163–75.
- 498 4. Beldjilali-Labro M, Garcia Garcia A, Farhat F, Bedoui F, Grosset J-F, Dufresne M, et al.
499 Biomaterials in Tendon and Skeletal Muscle Tissue Engineering: Current Trends and
500 Challenges. *Mater Basel Switz.* 2018 Jun 29;11(7).

- 1
2
3 501 5. Kishan AP, Cosgriff-Hernandez EM. Recent advancements in electrospinning design for
4 502 tissue engineering applications: A review. *J Biomed Mater Res A*. 2017
5 503 Oct;105(10):2892–905.
- 6
7
8 504 6. Lee NM, Erisken C, Iskratsch T, Sheetz M, Levine WN, Lu HH. Polymer fiber-based
9 505 models of connective tissue repair and healing. *Biomaterials*. 2017;112:303–12.
- 10
11 506 7. Maffulli N, Longo UG, Loppini M, Spiezia F, Denaro V. New options in the management
12 507 of tendinopathy. *Open Access J Sports Med*. 2010 Mar 31;1:29–37.
- 13
14
15 508 8. Magnusson SP, Langberg H, Kjaer M. The pathogenesis of tendinopathy: balancing the
16 509 response to loading. *Nat Rev Rheumatol*. 2010;6(5):262–8.
- 17
18 510 9. Andersson T, Eliasson P, Hammerman M, Sandberg O, Aspenberg P. Low-level
19 511 mechanical stimulation is sufficient to improve tendon healing in rats. *J Appl Physiol*
20 512 *Bethesda Md 1985*. 2012 Nov;113(9):1398–402.
- 21
22
23 513 10. Eliasson P, Andersson T, Aspenberg P. Influence of a single loading episode on gene
24 514 expression in healing rat Achilles tendons. *J Appl Physiol Bethesda Md 1985*. 2012
25 515 Jan;112(2):279–88.
- 26
27
28 516 11. Humphrey JD, Dufresne ER, Schwartz MA. Mechanotransduction and extracellular
29 517 matrix homeostasis. *Nat Rev Mol Cell Biol*. 2014 Dec;15(12):802–12.
- 30
31 518 12. Lee J, Guarino V, Gloria A, Ambrosio L, Tae G, Kim YH, et al. Regeneration of Achilles'
32 519 tendon: the role of dynamic stimulation for enhanced cell proliferation and mechanical
33 520 properties. *J Biomater Sci Polym Ed*. 2010;21(8–9):1173–90.
- 34
35
36 521 13. Engebretson B, Mussett ZR, Sikavitsas VI. Tenocytic extract and mechanical stimulation
37 522 in a tissue-engineered tendon construct increases cellular proliferation and ECM
38 523 deposition. *Biotechnol J*. 2017 Mar;12(3).
- 39
40
41 524 14. Engebretson B, Mussett ZR, Sikavitsas VI. The effects of varying frequency and duration
42 525 of mechanical stimulation on a tissue-engineered tendon construct. *Connect Tissue*
43 526 *Res*. 2018;59(2):167–77.
- 44
45 527 15. Li X, Zhang Y, Qi G. Evaluation of isolation methods and culture conditions for rat bone
46 528 marrow mesenchymal stem cells. *Cytotechnology*. 2013 May;65(3):323–34.
- 47
48
49 529 16. Neidert MR, Lee ES, Oegema TR, Tranquillo RT. Enhanced fibrin remodeling in vitro
50 530 with TGF-beta1, insulin and plasmin for improved tissue-equivalents. *Biomaterials*.
51 531 2002 Sep;23(17):3717–31.
- 52
53 532 17. Marturano JE, Arena JD, Schiller ZA, Georgakoudi I, Kuo CK. Characterization of
54 533 mechanical and biochemical properties of developing embryonic tendon. *Proc Natl*
55 534 *Acad Sci*. 2013 Apr 16;110(16):6370–5.

- 1
2
3 535 18. Gholipour Kanani A, Bahrami SH. Effect of Changing Solvents on Poly(ϵ -Caprolactone)
4 536 Nanofibrous Webs Morphology [Internet]. Journal of Nanomaterials. 2011 [cited 2020
5 537 Feb 12]. Available from: <https://www.hindawi.com/journals/jnm/2011/724153/>
6
7
8 538 19. Stoilov I, Starcher BC, Mecham RP, Broekelmann TJ. Chapter 7 - Measurement of
9 539 elastin, collagen, and total protein levels in tissues. In: Mecham RP, editor. Methods in
10 540 Cell Biology [Internet]. Academic Press; 2018 [cited 2020 Feb 12]. p. 133–46. (Methods
11 541 in Extracellular Matrix Biology; vol. 143). Available from:
12 542 <http://www.sciencedirect.com/science/article/pii/S0091679X17301292>
13
14
15 543 20. Ikoma K, Kido M, Nagae M, Ikeda T, Shirai T, Ueshima K, et al. Effects of stress-shielding
16 544 on the dynamic viscoelasticity and ordering of the collagen fibers in rabbit Achilles
17 545 tendon. J Orthop Res Off Publ Orthop Res Soc. 2013 Nov;31(11):1708–12.
18
19
20 546 21. Bölgen N. 10 - Electrospun materials for bone and tendon/ligament tissue engineering.
21 547 In: Uyar T, Kny E, editors. Electrospun Materials for Tissue Engineering and Biomedical
22 548 Applications [Internet]. Woodhead Publishing; 2017 [cited 2020 Feb 12]. p. 233–60.
23 549 Available from:
24 550 <http://www.sciencedirect.com/science/article/pii/B9780081010228000041>
25
26
27 551 22. Martin RB, Burr DB, Sharkey NA, Fyhrie DP. Mechanical Properties of Ligament and
28 552 Tendon. In: Martin RB, Burr DB, Sharkey NA, Fyhrie DP, editors. Skeletal Tissue
29 553 Mechanics [Internet]. New York, NY: Springer; 2015 [cited 2020 Feb 12]. p. 175–225.
30 554 Available from: https://doi.org/10.1007/978-1-4939-3002-9_4
31
32
33 555 23. Choi K-M, Seo Y-K, Yoon H-H, Song K-Y, Kwon S-Y, Lee H-S, et al. Effects of mechanical
34 556 stimulation on the proliferation of bone marrow-derived human mesenchymal stem
35 557 cells. Biotechnol Bioprocess Eng. 2007 Dec 1;12(6):601–9.
36
37
38 558 24. Kuang R, Wang Z, Xu Q, Liu S, Zhang W. Influence of mechanical stimulation on human
39 559 dermal fibroblasts derived from different body sites. Int J Clin Exp Med.
40 560 2015;8(5):7641–7.
41
42 561 25. Xu Y, Dong S, Zhou Q, Mo X, Song L, Hou T, et al. The effect of mechanical stimulation
43 562 on the maturation of TDSCs-poly(L-lactide-co-e-caprolactone)/collagen scaffold
44 563 constructs for tendon tissue engineering. Biomaterials. 2014 Mar;35(9):2760–72.
45
46
47 564 26. Wang Y-K, Chen CS. Cell adhesion and mechanical stimulation in the regulation of
48 565 mesenchymal stem cell differentiation. J Cell Mol Med. 2013 Jul;17(7):823–32.
49
50 566 27. Subramony SD, Dargis BR, Castillo M, Azeloglu EU, Tracey MS, Su A, et al. The guidance
51 567 of stem cell differentiation by substrate alignment and mechanical stimulation.
52 568 Biomaterials. 2013 Mar;34(8):1942–53.
53
54
55 569 28. Screen HRC, Shelton JC, Bader DL, Lee DA. Cyclic tensile strain upregulates collagen
56 570 synthesis in isolated tendon fascicles. Biochem Biophys Res Commun. 2005 Oct
57 571 21;336(2):424–9.
58
59
60

- 1
2
3 572 29. Huisman E, Lu A, McCormack RG, Scott A. Enhanced collagen type I synthesis by human
4 573 tenocytes subjected to periodic in vitro mechanical stimulation. *BMC Musculoskelet*
5 574 *Disord.* 2014 Nov 21;15:386.
- 6
7
8 575 30. Wu S, Wang Y, Streubel PN, Duan B. Living nanofiber yarn-based woven biotextiles for
9 576 tendon tissue engineering using cell tri-culture and mechanical stimulation. *Acta*
10 577 *Biomater.* 2017 15;62:102–15.
- 11
12 578 31. Heinemeier KM, Kjaer M. In vivo investigation of tendon responses to mechanical
13 579 loading. *J Musculoskelet Neuronal Interact.* 2011 Jun;11(2):115–23.
- 14
15
16 580 32. Dex S, Alberton P, Willkomm L, Söllradl T, Bago S, Milz S, et al. Tenomodulin is Required
17 581 for Tendon Endurance Running and Collagen I Fibril Adaptation to Mechanical Load.
18 582 *EBioMedicine.* 2017 Jun;20:240–54.
- 19
20
21 583 33. Nagasawa K, Noguchi M, Ikoma K, Kubo T. Static and dynamic biomechanical
22 584 properties of the regenerating rabbit Achilles tendon. *Clin Biomech Bristol Avon.* 2008
23 585 Jul;23(6):832–8.
- 24
25 586 34. Doroski DM, Brink KS, Temenoff JS. Techniques for biological characterization of tissue-
26 587 engineered tendon and ligament. *Biomaterials.* 2007 Jan;28(2):187–202.
- 27
28
29 588 35. Kubo K, Kanehisa H, Fukunaga T. Effect of stretching training on the viscoelastic
30 589 properties of human tendon structures in vivo. *J Appl Physiol Bethesda Md* 1985. 2002
31 590 Feb;92(2):595–601.
- 32
33 591 36. Licup AJ, Münster S, Sharma A, Sheinman M, Jawerth LM, Fabry B, et al. Stress controls
34 592 the mechanics of collagen networks. *Proc Natl Acad Sci U S A.* 2015 Aug
35 593 4;112(31):9573–8.
- 36
37
38 594 37. Martin RB, Ishida J. The relative effects of collagen fiber orientation, porosity, density,
39 595 and mineralization on bone strength. *J Biomech.* 1989;22(5):419–26.

40 596

41 597

42 598

43
44
45
46
47
48 599 **Author contributions**

49 600 A.G.G conceived, designed and performed the experiments. J.B.P developed the mechanical
50 601 data analysis and assisted with in vitro mechanical stimulation. M.B.L was involved with cell
51 602 culture maintain. S.L.R and M.N provided support and information regarding cell extraction.
52
53 603 Q.D provided technical support with Bose BioDynamic 5100. C.L and F.B provides scientific
54
55 604 directions and analysis of the data. A.G.G, C.L and F.B wrote the manuscript.
56
57
58
59 605

1
2
3 606 **Competing interests**

4
5 607 The authors declare no competing interests.
6
7 608

8
9 609 **Figure legends**

10 610 **Figure 1.** Electrospinning device.

11
12 611 **Figure2.** Experimental plan design. Correlation between cellular activity (Cell Scale T6) and
13 612 biomechanical performance (Bose Biodynamic 5100).

14 613 **Figure3.** SEM pictograph of a 10-wt % PCL scaffold **(A)**. Fibre orientation distribution in PCL
15 614 scaffolds **(B)**.

16 615 **Figure 4.** Stress (MPa) vs strain (%) curve for 10-wt % PCL scaffolds in a dry (dark grey) or
17 616 wet (light grey) state, obtained using the Electroforce 3200 system.

18 617 **Figure 5.** Cell proliferation (#) and hydroxyproline synthesis (\$) over time, at 1 and 2 weeks
19 618 of

20 619 static and dynamic culture performed with T6 CellScale. Hydroxyproline concentration was
21 620 related to collagen content (***) for $p < 0.001$. (*) Fluorescence staining of the actin
22 621 cytoskeleton (red) (A-D), type-1 collagen (green) (E-F) and tendomodulin (I-L) for static or
23 622 dynamic culture performed for 1 or 2 weeks). Cell nuclei were stained blue as a counter-
24 623 stain.

25 624 Scale bar of 50 μ m.

26 625 **Figure 6.** Design of the dynamic culture process during 12 days of stimulation **(A)**.
27 626 Representative stress vs strain curve **(B)** of the first sinus from the first cycle and the last
28 627 sinus from the last cycle for cell-constructs subjected to dynamic culture conditions.

29 628 **Figure 7.** Tan δ , Energy dissipation values, E^* , E' and E'' for both dynamic and static
30 629 conditions cultured with or without cells for both days 2 and 14. Tests were performed in
31 630 the Bose BioDynamic 5100. Values represent the arithmetic average for each value from
32 631 1200 to 3600 sinuses ($n=3$). There was no statistical difference between the conditions.

33 632 **Figure 8.** Evolution of the Tan δ **(A)**, dissipated energy **(B)**, E' **(C)** and E'' **(D)** over time
34 633 expressed in terms of variation (V%). $V\% = ((\text{Last cycle} - \text{First cycle}) / (\text{First cycle})) * 100$.

35 634 **Figure 9.** Schematic representation of evolution in the mechanical properties for cellular
36 635 constructions in the absence or presence of mechanical stimulation.

1
2
3 636
4
5
6 637
7
8
9 638
10
11 639
12
13 640
14
15 641
16
17 642
18
19 643
20
21 644
22
23 645
24
25 646
26
27 647
28
29 648
30
31 649
32
33 650
34
35 651
36
37 652
38
39
40
41
42
43
44
45
46
47
48
49
50
51
52
53
54
55
56
57
58
59
60

For Peer Review

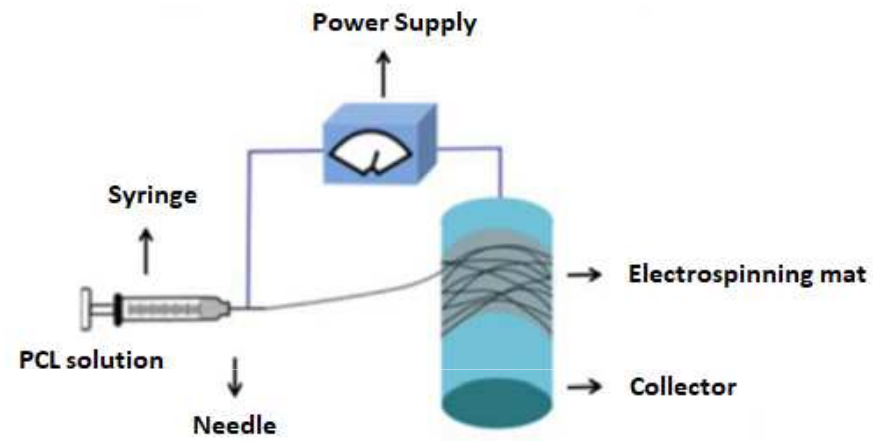


Figure 1. Electrospinning device.

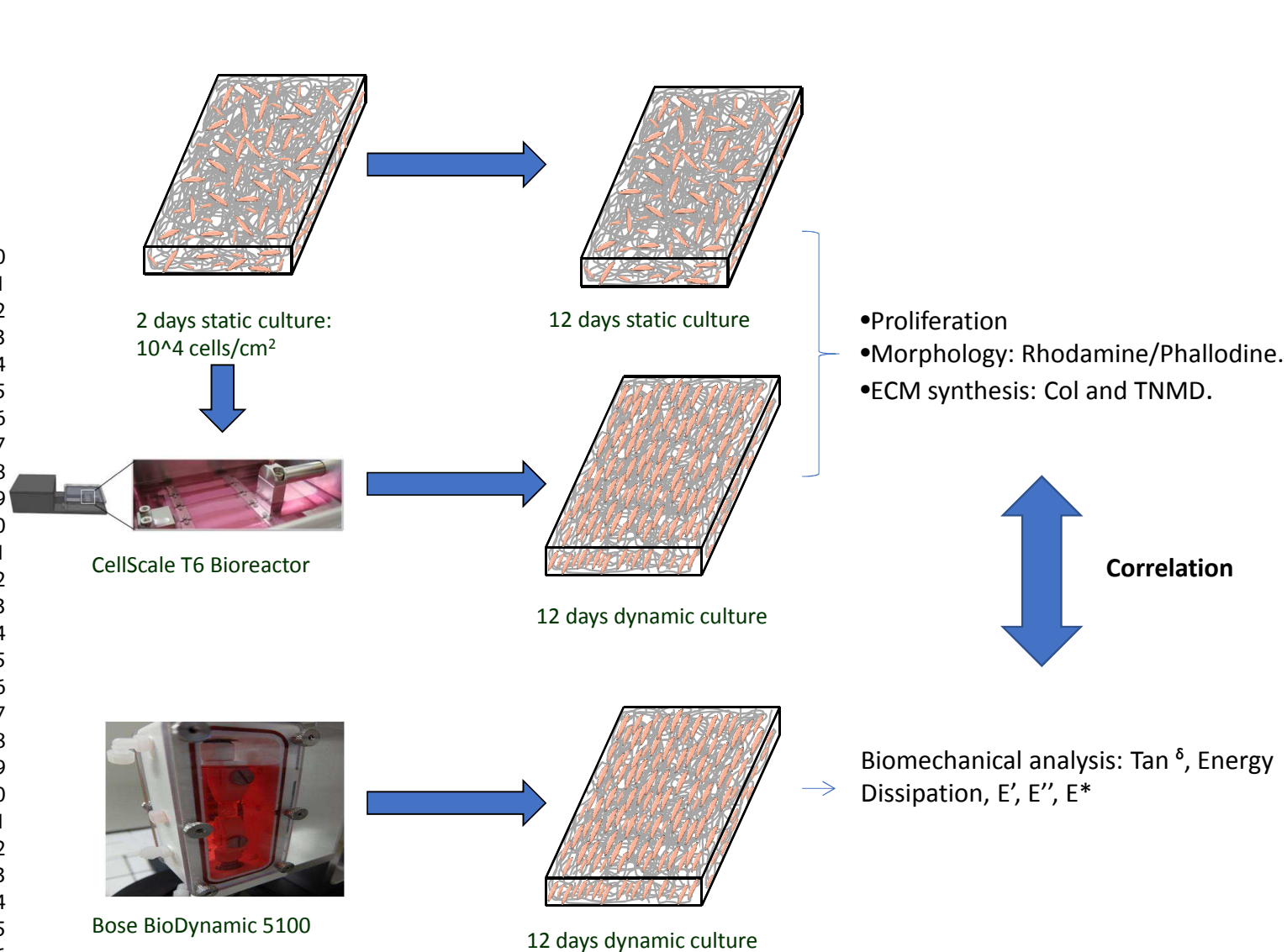


Figure 2. Experimental plan design. Correlation between cellular activity (Cell Scale T6) and biomechanical performance (Bose Biodynamic 5100). Briefly, after 2 days of static culture, scaffolds were transferred to the different bioreactors (Electro Force and Bose Biodynamic). Once attached, the dynamic culture was launched for 2 weeks.

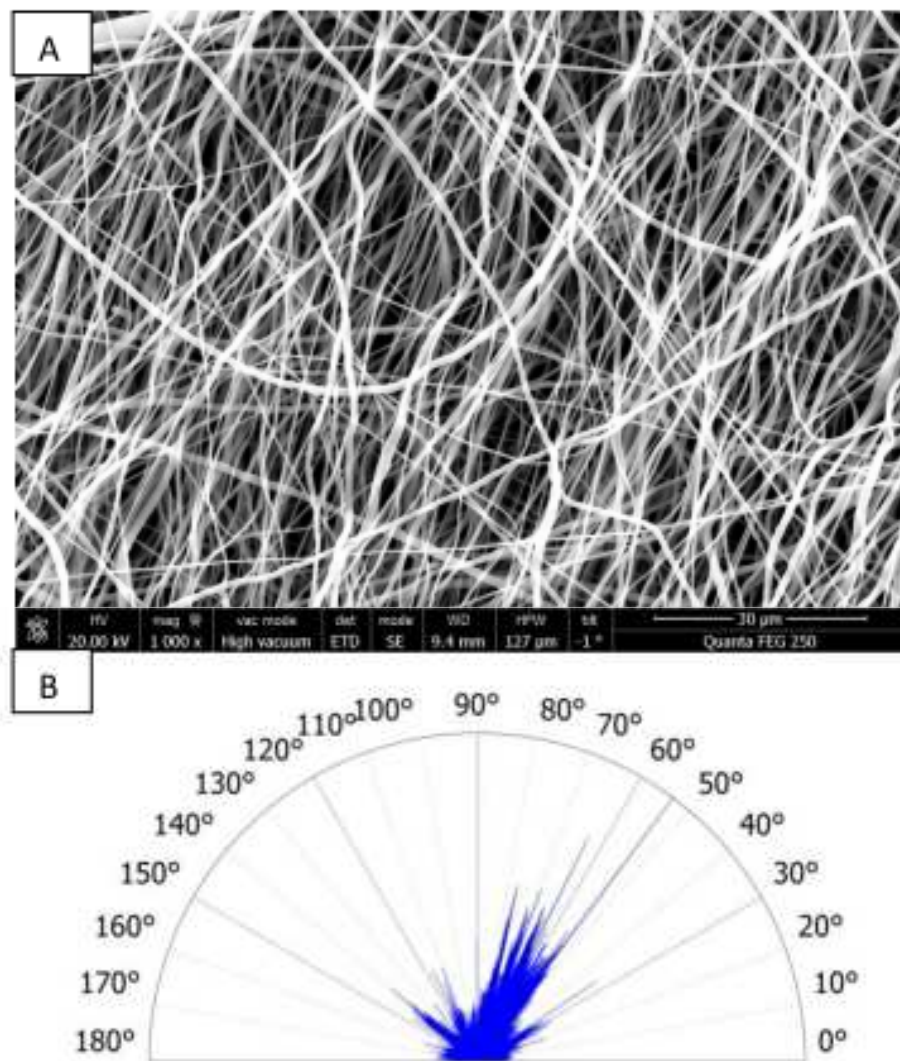


Figure 3. SEM pictograph of a 10-wt % PCL scaffold **(A)**. Fibre orientation distribution in PCL scaffolds **(B)**.

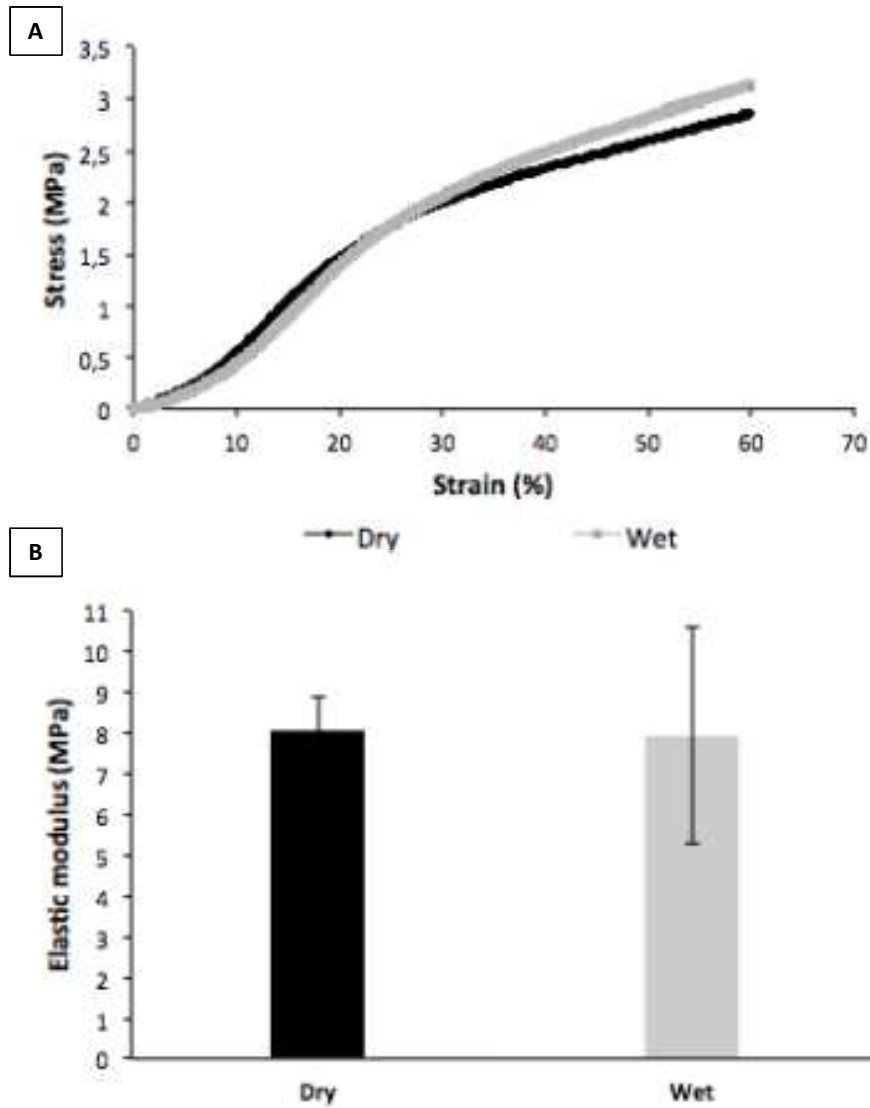


Figure 4. Stress (MPa) vs strain (%) curve for 10-wt % PCL scaffolds in a dry (dark grey) or wet (light grey) state, obtained using the Electroforce 3200 system.

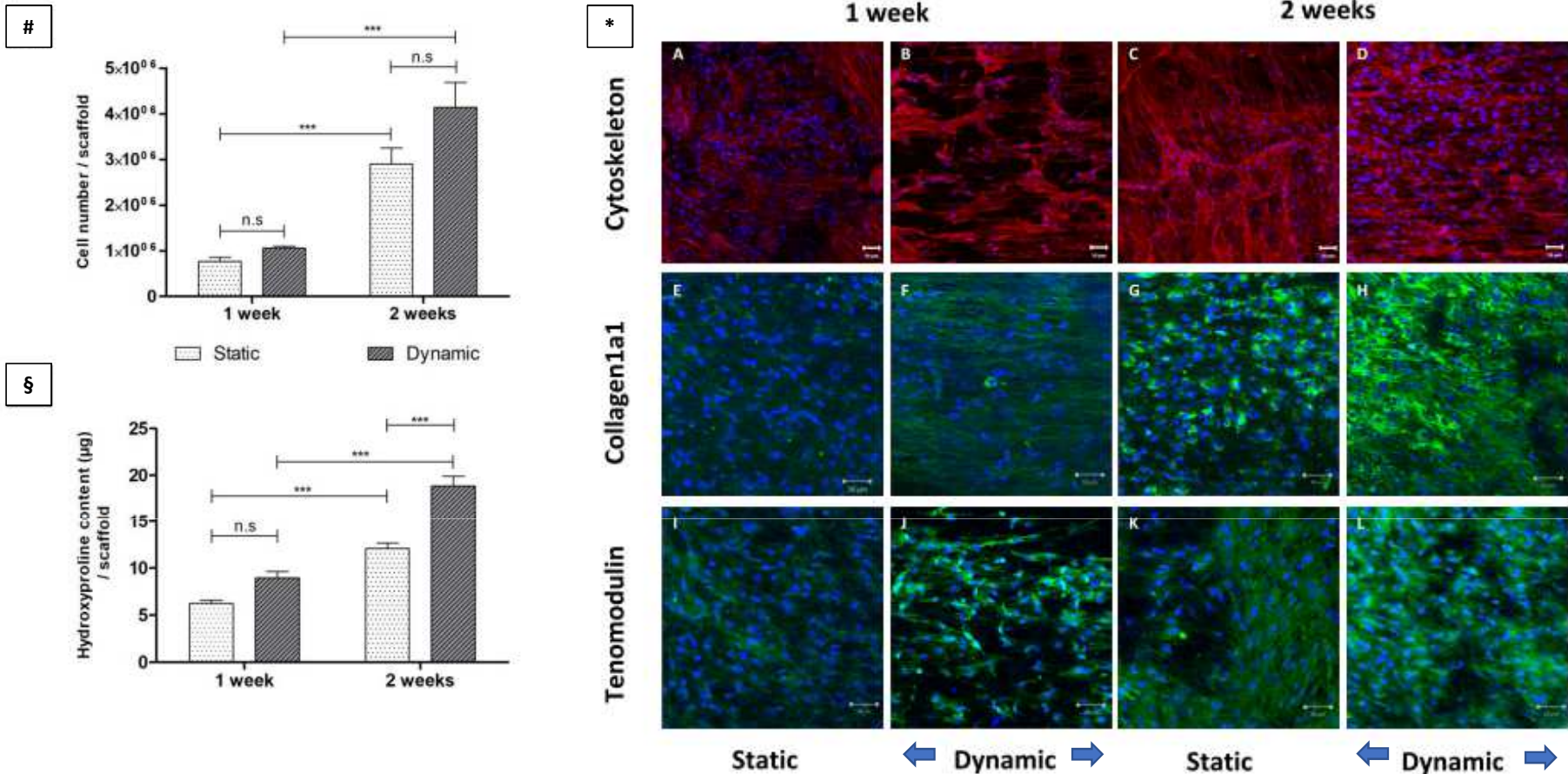


Figure 5. Cell proliferation (#) and hydroxyproline synthesis (§) over time, at 1 and 2 weeks of static and dynamic culture performed with T6 CellScale. Hydroxyproline concentration was related to collagen content (***) for p<0.001. (*) Fluorescence staining of the actin cytoskeleton (red) (A-D), type-1 collagen (green) (E-F) and tendomodulin (I-L) for static or dynamic culture performed for 1 or 2 weeks). Cell nuclei were stained blue as a counter-stain. Scale bar of 50µm. Blue arrows indicate the sense of the stretch.

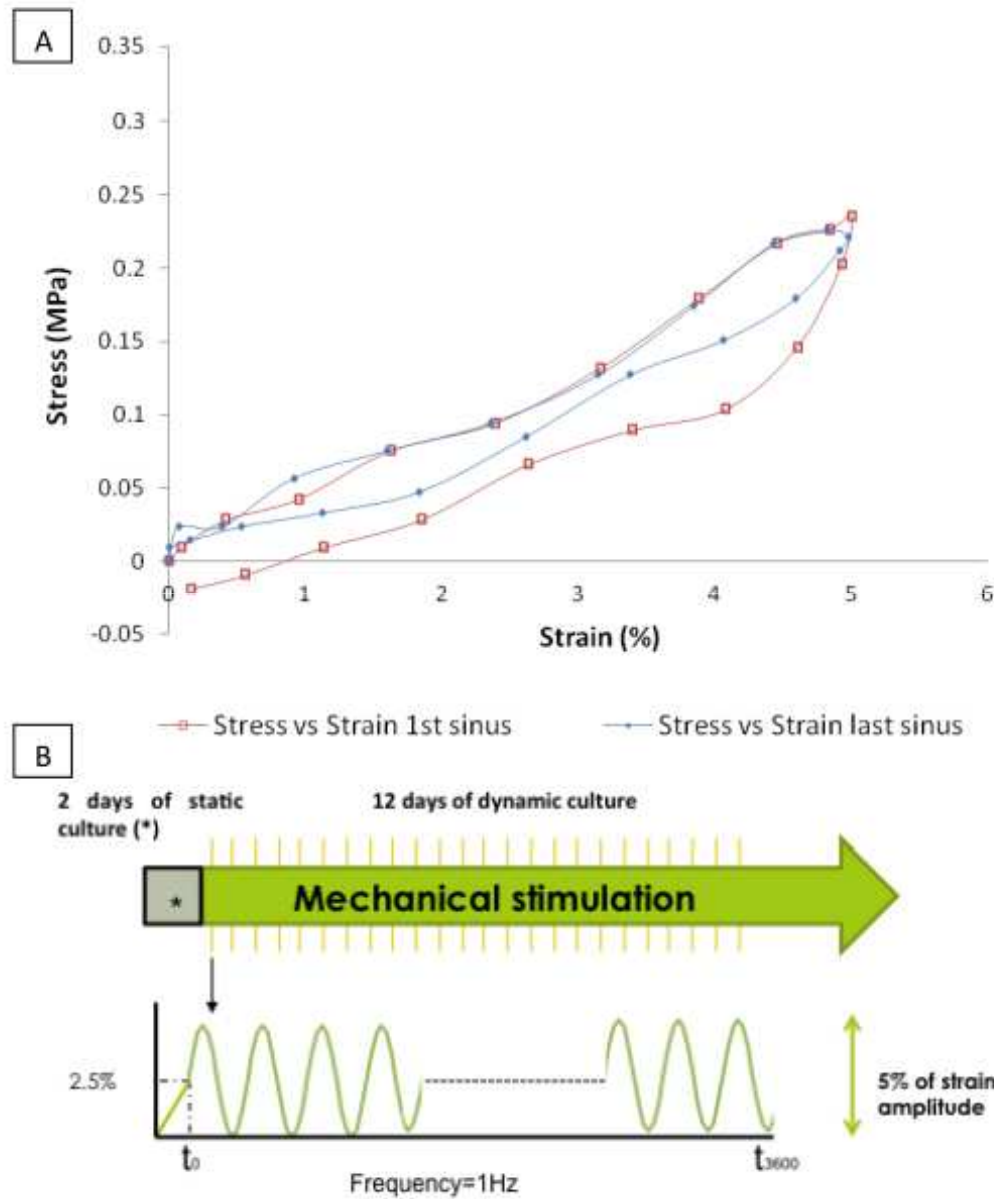


Figure 6. Design of the dynamic culture process during 12 days of stimulation **(A)**. Representative stress vs strain curve **(B)** of the first sinus from the first cycle and the last sinus from the last cycle for cell-constructs subjected to dynamic culture conditions. After 2 days of static culture, the cell-construct or the control scaffolds were fixed inside the bioreactor chamber and the mechanical test was launched. Both signal force and displacement were recorded over time and found to be smooth, without any background noise, making it possible to monitor mechanical (elastic and viscoelastic) properties.

	Tan delta		Hysteresis		E* (MPa)		E' (MPa)		E'' (MPa)	
	2 days	14 days	2 days	14 days	2 days	14 days	2 days	14 days	2 days	14 days
Static with cells	0.08± 0.01	0.10± 0.01	0.64± 0.35	0.80± 0.14	3.97± 2.27	4.27± 0.79	3.95± 2.26	4.24± 0.78	0.30± 0.16	0.44± 0.08
Static control	0.12± 0.03	0.12± 0.02	0.92± 0.14	0.81± 0.11	4.03± 0.92	3.46± 0.43	3.90± 0.91	3.42± 0.43	0.42± 0.07	0.38± 0.06
Dynamic with cells	0.09± 0.01	0.10± 0.06	0.90± 0.11	1.02± 0.12	4.34± 1.21	5.07± 0.11	4.32± 1.20	5.04± 0.11	0.37± 0.13	0.49± 0.02
Dynamic control	0.09± 0.03	0.09± 0.03	1.47± 0.57	1.32± 0.48	6.68± 0.87	6.24± 0.83	6.63± 0.89	6.21± 0.84	0.59± 0.14	0.53± 0.10

Figure 7. Tan δ , Energy dissipation values, E*, E' and E'' for both dynamic and static conditions cultured with or without cells for both days 2 and 14. Tests were performed in the Bose BioDynamic 5100. Values represent the arithmetic average for each value from 1200 to 3600 sinuses (n=3). There was no statistical difference between the conditions.

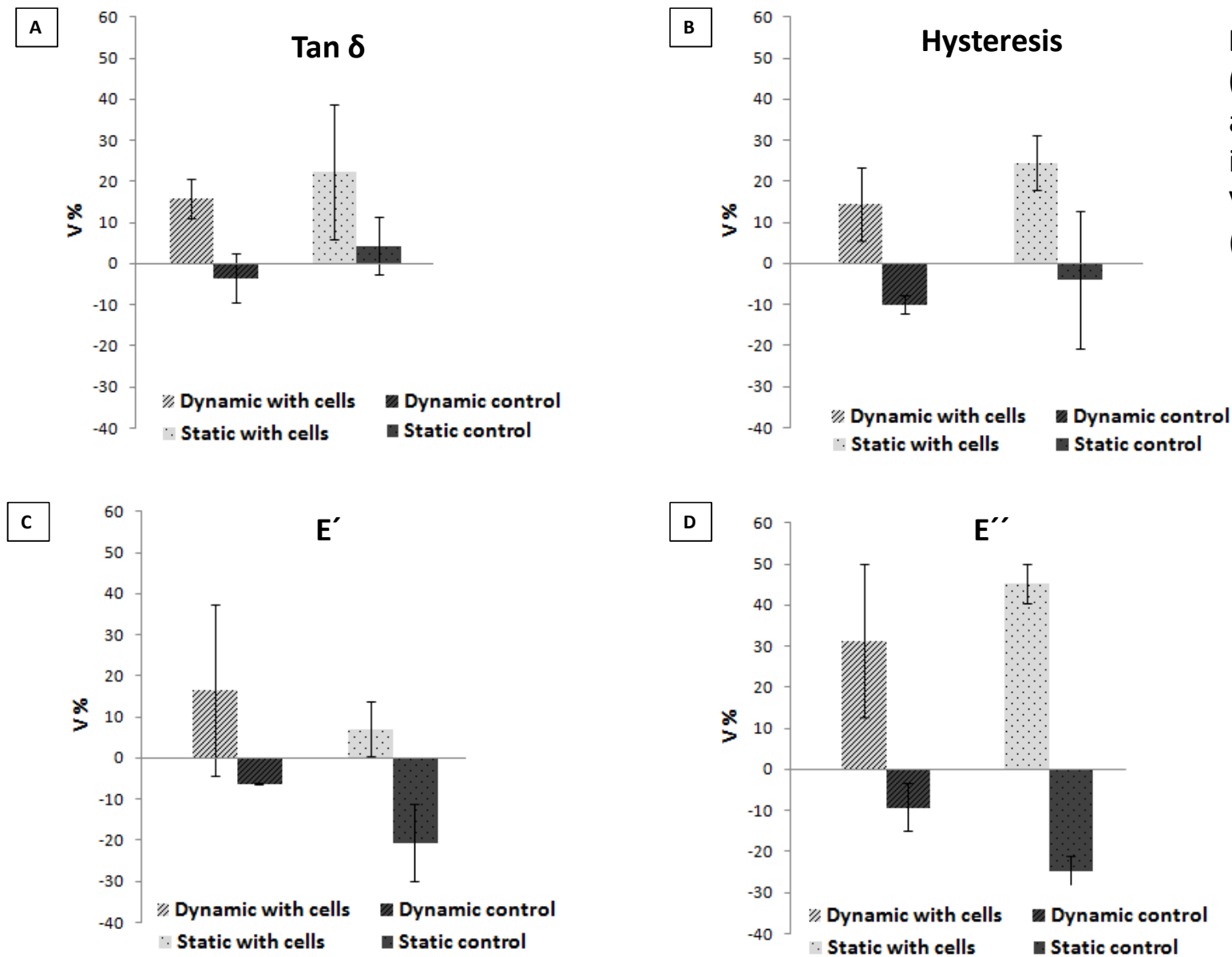
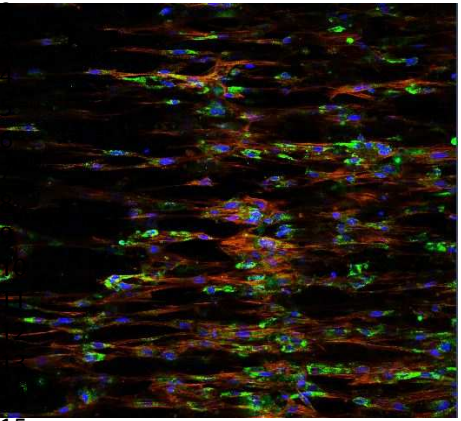
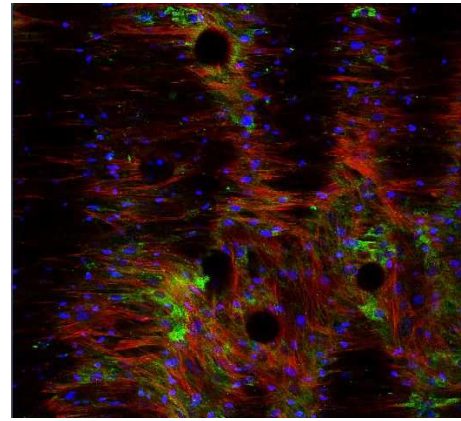
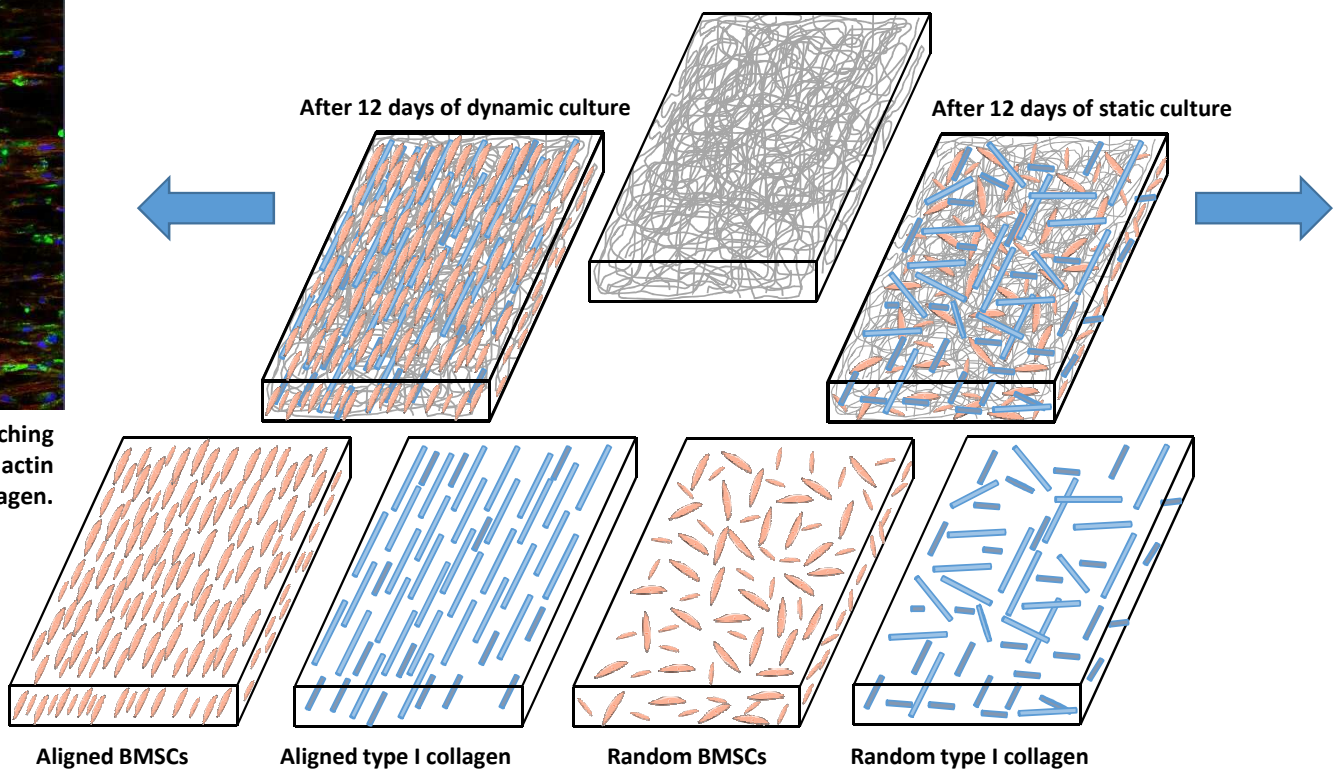


Figure 8. Evolution of the Tan δ (A), dissipated energy (B), E' (C) and E'' (D) over time expressed in terms of variation (V%). $V\% = ((\text{Last cycle} - \text{First cycle}) / (\text{First cycle})) * 100$

1



15 Aligned cells along the stretching
16 direction. Blue: cells nuclei; red: actin
17 cytoskeleton; green: type I collagen.
18 Single stack image.
19



20 Randomly organized cells. Blue: cells
21 nuclei; red: actin cytoskeleton; green:
22 type I collagen. Single stack image.
23
24
25
26
27
28
29

	Tan delta	E'	E''
Static with cells	↑↑	↑	↑↑
Dynamic with cells	↑	↑↑	↑

30
31
32
33
34
35
36
37
38
39
40
41
42
43
44
45
46
Figure 9. Schematic representation of evolution in the mechanical properties for cellular constructions in the absence or presence of mechanical stimulation.